EDGE WELD PENETRATION ASSESSMENT VIA ELECTRIC CURRENT DEFLECTION MEASUREMENTS

Shaohai Chen and Peter B. Nagy
Department of Aerospace Engineering
University of Cincinnati
Cincinnati, Ohio 45221-0070

INTRODUCTION

Because of the awkward and somewhat irregular shape of the weldment, conventional methods [1] could not be adapted to the nondestructive measurement of GTAW edge weld penetration on clamshell-style catalytic converters and a special inspection system based on the electric current deflection method was developed. DC or low-frequency AC electric resistance measurements, also known as the Potential Drop Method (PDM), are well-developed for plate thickness assessment and crack detection [2-6]. The operating principle of these methods is that, under certain arrangement of the electrodes, the defect or crack in a conducting specimen will cause a measurable increase in resistance between given points compared to the situation without the defect or crack. In recent years, this simple contact technique was largely obscured by more sophisticated noncontacting eddy-current techniques especially in industrial applications. In this article, we demonstrate the distinct advantages of the Potential Drop Method through the example of GTAW edge welds where the awkward shape of the specimens and the required large penetration depth render the eddy-current method less feasible.

Figure 1 shows the schematic diagram of an edge weld. The weld penetration w is defined as the distance from the tip of the crack separating the welded plates to the nearest point on the contour of the weld bead. This point is usually, but not necessarily straight ahead at the virtual extension of the crack to the contour. Typically, a good weld has a penetration of at least 60% of the plate thickness, i.e., $w \geq 0.6d$. The electric resistance through the edge-welded flange is strongly affected by the weld penetration. However, the intrinsic electrical resistance of the weld is usually very small compared to the contact resistance between the plate and the measuring electrodes. Therefore, a four-point electric resistance measurement technique is used to reduce the adverse effect of the contact resistance [2]. We used finite element analysis to simulate the current distribution in the weld [5] in order to estimate the relationship between the sought penetration depth and the measured electrical resistance, to optimize the electrode arrangement, and to estimate the adverse effects of spurious geometrical variations in the weld shape.

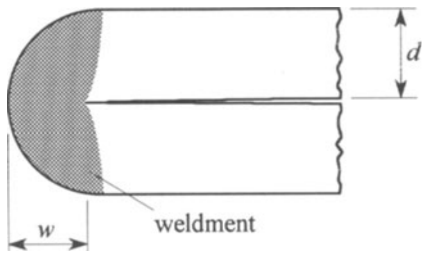

Figure 1 Schematic diagram of an edge weld.

NUMERICAL RESULTS

Although the operating principle of PDM is simple, the interpretation of the measurements can be very complex. Calibration curves for defects in flat plate configuration using either uniform constant current arrangement or four-point probe arrangement have been generated by analytical [7], numerical [8, 9], and experimental [2] methods. However, these results cannot be directly applied to obtain the solution for a specimen of complicated geometry shown in Fig. 1. In order to simulate the current distribution in GTAW edge welds, the commercial ANSYS5.2 finite element program was used [10]. Since the governing equations for both electrostatic and steady-state heat transfer problems are similar Laplace or Poisson equations, an analogy between them can be exploited [11]. Instead of directly solving the electrostatic problem, we solved the analogous steady-state heat transfer problem which is fully supported by ANSYS5.2.

Figure 2 shows the physical model used in our finite element calculations. The main assumptions in this model are that (1) the resistivity of the material is uniform, (2) the conductivity of the weldment is the same as that of the base material and (3) the electrical conductance through the compressed but unbonded crack tip is negligible [2]. The potential distribution was calculated in three dimensions. In order to simulate the actual case, the edge effects should be eliminated. We found that the deviations due to edge effects are less than 1% provided that the length L and width W of the model are greater than 0.440" and 0.520", respectively. Subsequently, we set $L = W = 0.800''$ in all of our calculations to eliminate the edge effect. The distance between the current injection point to the tip of the weld is not critical in our case. We set it as $i = 0.160''$ while the plate thickness is $d = 0.060''$. The position of the sensing electrodes does not affect the potential distribution, therefore the transfer resistance for different sensing electrode locations can be determined from the same calculation. From the calculated potential difference between the two points of the sensing electrodes and the value of the injected electrical current, we can determine the transfer resistance of different weld geometries and dimensions. This method was successfully used to simulate the operation of the electrical current deflectometer in a way which would have been extremely difficult to do experimentally.

Figure 3 shows the electric resistance versus weld penetration curves for three different sensor stand-off distances. The symbols are finite element results and the solid lines are best fitting polynomial approximations. The measuring characteristics can be greatly linearized by positioning the sensing electrodes at a larger distance from the tip of the weld. However, the measuring sensitivity also decreases as the relative contribution of the weld resistance in the measured total resistance becomes smaller with respect to the increasing contribution from the base plate. An additional limitation on positioning the sensing electrodes is the often badly oxidized surface of the weldment, which makes the electrode contact somewhat

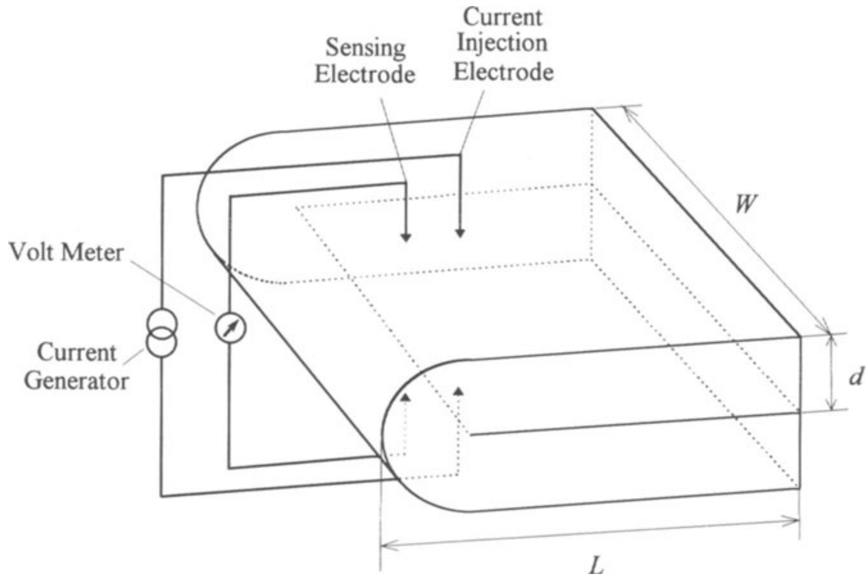

Figure 2 Schematic picture of the physical model and the electrical arrangement for PDM measurements.

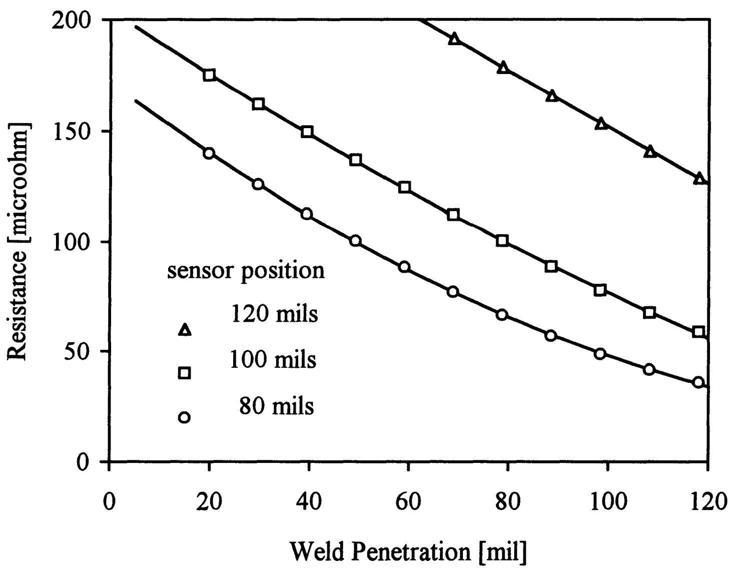

Figure 3 Electric resistance versus weld penetration for three different sensor stand-off distances. The symbols are Finite Element results and the solid lines are best fitting polynomial approximations (plate thickness 0.060", injector stand-off 0.160", resistivity 56.6 μΩcm).

uncertain. Therefore, the minimum stand-off distance of the sensing electrodes from the weld tip is about 0.070-0.080″ when sharp steel pins are used to pierce through the contamination. In the case of less effective but more convenient spring-loaded electrodes, the minimum stand-off distance is much higher on the order of 0.15-0.20″ depending on how well the shielding gas protected the surface from oxidization.

Figure 4 demonstrates the lateral resolution of the electric current deflectometer for two different sensor stand-off distances. In this calculation we assumed that the penetration depth abruptly changes from 0.050" on the left side to 0.030" on the right. Because the electric current fans out considerably in the lateral direction, this abrupt transition is significantly smoothened as the resistance sensor is moved over the transition region. Until approximately 0.125" away from the transition the current deflectometer doesn't measure the weld penetration directly in front of it. If the sensor is placed closer to the transition, the resistance will be affected by the penetration depth on the other side of the transition. Directly over the transition, the measured resistance, i.e., the predicted penetration depth, is roughly the average of the two sides. The abrupt change in the penetration depth is recorded as a continuous transition from the constant value on one side to the other constant value on the other side. Based on these results, the lateral resolution of the current deflectometer is approximately 0.250". This smoothening feature makes the electrical resistance technique especially suitable to monitor trends in the weld penetration as the basically random local variations are effectively eliminated from the measurement.

The finite element simulation technique can be also readily used to estimate the adverse affect of changing weld bead shape on the accuracy of the weld penetration assessment from electrical resistance measurement. One typical kind of shape distortion is shown in Figure 5. Although the surface tension of the molten material often assures that the weld

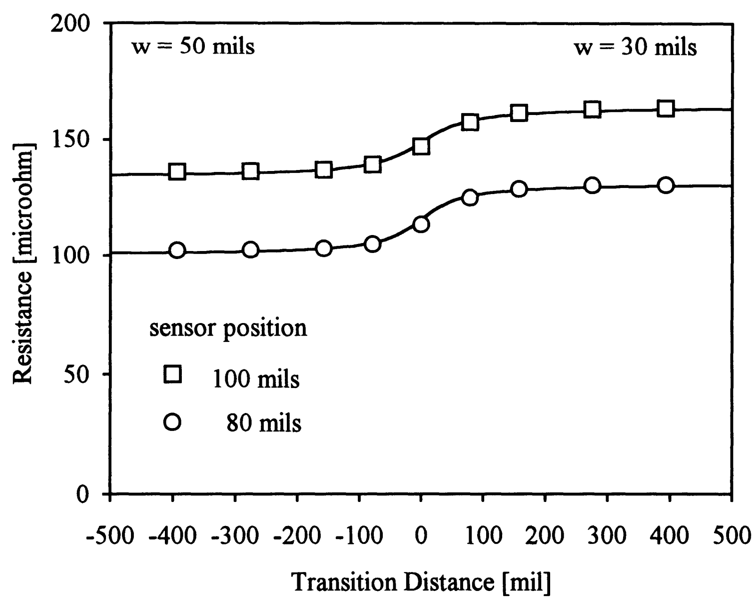

Figure 4 Illustration of the lateral resolution of the electric current deflectometer for two different sensor stand-off distances (plate thickness 60 mils, injector stand-off 160 mils, resistivity 56.6 $\mu\Omega$cm).

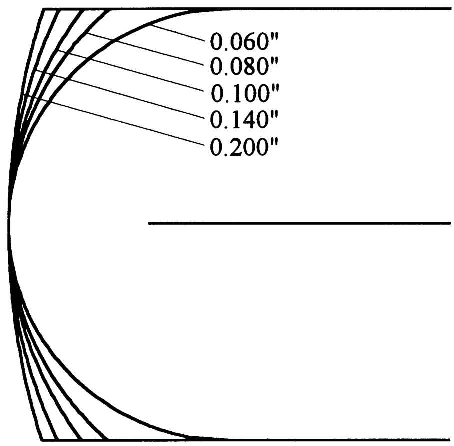

Figure 5 Typical distortion of the weld bead shape caused by increasing radius of curvature (plate thickness 0.060", weld penetration 0.040").

shape is essentially cylindrical, the radius of the weld bead can be larger than the plate thickness so that the weldment appears to be slightly flattened with respect to the ideal circular cross section and a more or less sharp contour line is formed between the surfaces of the weld bead and the base plate. Figure 6 shows the electric resistance versus beam radius for two different sensor stand-off distances as predicted by our finite element calculations (plate thickness 0.060", weld penetration 0.040", injector stand-off 0.160", resistivity 56.6 μΩcm). As one would expect, the weld resistance slightly decreases with

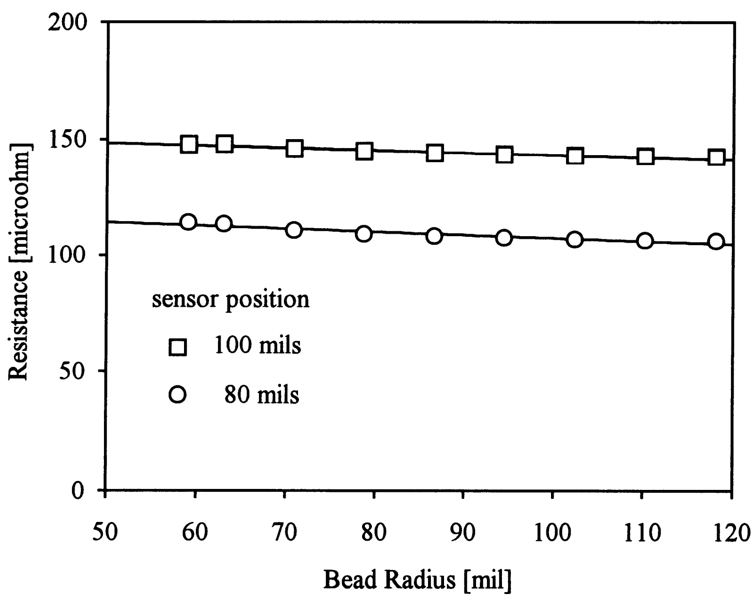

Figure 6 Electric resistance versus beam radius for two different sensor stand-off distances (plate thickness 0.060", weld penetration 0.040", injector stand-off 0.160", resistivity 56.6 μΩcm).

increasing radius of curvature since the "added" material, although it is not in the region of high current density, still reduces the resistance for the same penetration depth. The drop in weld resistance as the radius increases from 0.060" to 0.120" is approximately 10%, i.e., a relatively small fraction, therefore the accuracy of the weld penetration assessment is not compromised significantly.

Of course the finite element technique can be used to calculate the resistance of practically any awkward shaped weldments therefore it is especially well suited to study the effect of weld geometry in a statistical way using actual specimen geometries chosen from a large set of manufactured products. By doing so, we found that distorted weld beads exhibit slightly lower electrical resistance for the same weld penetration in general. The main reason for this is that the peak of the weld is used as the reference point for positioning the electrodes therefore the electrodes are placed more forward with respect to the crack tip on distorted specimens. However, even among the worst cases chosen from a large set of specimens, the resistance reduction due to weld shape distortion is much less than 10% and the resulting overestimation of the weld penetration is acceptable.

EXPERIMENTAL VERIFICATION

We have developed an Electric Current Deflectometer and Computer Controlled Data Acquisition System based on the previously described principle to measure GTAW edge weld penetration on clamshell-style catalytic converters. The system is based on an LR-700 AC Resistance Bridge that measures the resistance of the edge weld using a special 4-point probe. The measured resistance value is transmitted via an RS232 interface to the Data Acquisition Computer, where a Windows 95 application program carries out the evaluation. We measured resistance at 14 different locations around the perimeter of the catalytic converter. Each measurement was repeated 5 times to establish the reproducibility of the measurement. The average resistance was 80.75 $\mu\Omega$ with a standard deviation of 2.19 $\mu\Omega$ which corresponds to 2.71 % relative variance. Most of this variance is due to mechanical uncertainties encountered when the measuring electrode is mounted on the converter. Considering the nature of the weld penetration assessment, the overall reproducibility of the measurement is quite sufficient.

Somewhat less accurate correlation was found by using metallurgical testing, which is the currently used in industry to measure the weld penetration on an everyday basis. Figure 7 shows the comparison between nondestructive and metallurgical measurements of the weld penetration. According to this practice, the specimens are first sectioned, mounted in bakelite, polished, chemically etched, then optically analyzed. This method is more susceptible to operator errors as tightly closed crack tips might avoid detection or surface cracks and grain boundaries might be mistakenly identified as cracks. Furthermore, large variations from point to point can occur in the weld penetration, which can be easily averaged out when measuring the width of the fracture surface, but cause inevitable errors when single sections are inspected.

Figure 8 shows another comparison between nondestructive and destructive measurements of the weld penetration. Here, the destructive data was obtained by optically measuring the width of the fracture surface after peel testing. Over a very wide range of weld penetration extending from 0.015" to 0.080", the nondestructive data very well correlate to the destructive results. These results suggest that the often used metallurgical sectioning technique is actually more susceptible to experimental uncertainties than the considerably simpler peel-off test with subsequent fracture surface analysis.

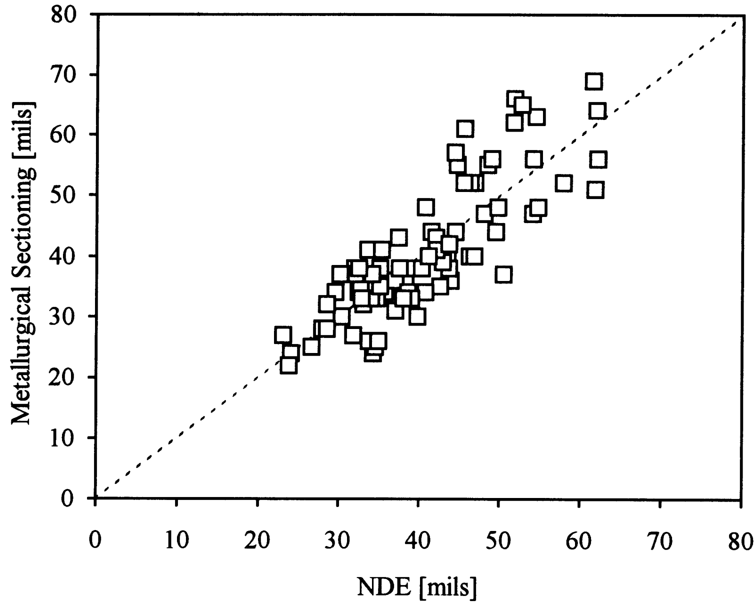

Figure 7 Comparison between nondestructive and metallurgical measurements of the weld penetration.

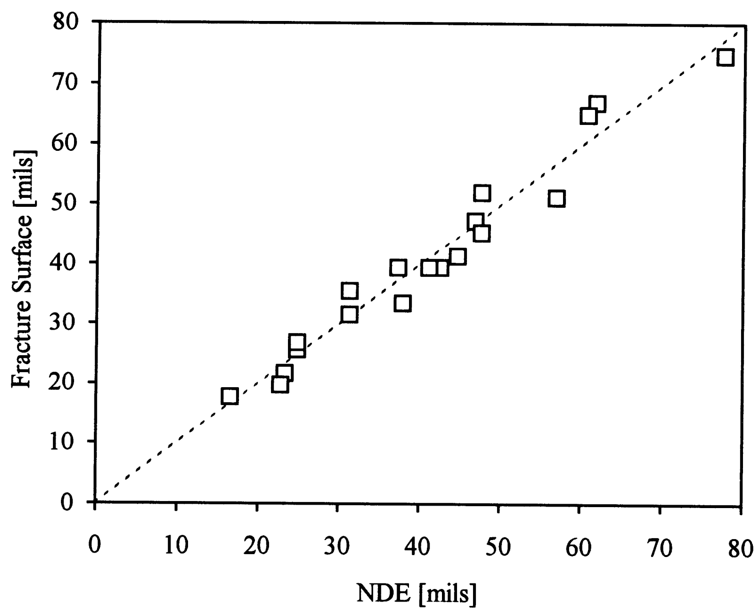

Figure 8 Comparison between nondestructive and destructive measurements of the weld penetration (via measuring the width of the fracture surface).

CONCLUSIONS

We developed a novel nondestructive technique for assessing the edge weld penetration on clamshell-style catalytic converters based on electrical resistivity measurement. Extensive numerical simulations using ANSYS5.2 finite element program were carried out to assess the current distribution in the weld so that an optimal electrode configuration could be found and the inevitable adverse effects of weld irregularities could be reduced. Our results indicated that the weld shape has but an acceptable effect on the weld penetration estimate. A special inspection system was developed based on these findings and the experimental results were found to be within approximately ± 10% of the destructive data obtained by fracturing the specimens. Comparison with metallurgical tests yielded a somewhat lower accuracy of ± 20%. This discrepancy should be further investigated. However, measurement of the width of the fracture surface appears to be a more reliable method to determine the weld penetration and can be directly correlated to peel strength, therefore the found good agreement with the nondestructive results clearly shows the potential of the developed technique for industrial applications.

The measurement of the weld penetration around the perimeter of the converter is fast, accurate, and reproducible. Due to technological difficulties, the weld penetration often varies as much as ±50%. The purpose of the weld penetration measurement is to establish the average and lowest values for the converter under inspection. Since only 14 points were actually tested, the inherent uncertainty about the average value is almost ±15% regardless how accurately we measured the penetration depth at the 14 locations. Similarly, depending on the probability distribution of the weld penetration, the minimum penetration depth determined based on 14 points might be much higher than the actual minimum around the perimeter of the converter. Because of these adverse effects, it is more desirable to increase the speed of the measurement and thereby the number of points actually measured than trying to measure with higher accuracy and reproducibility at the few randomly chosen locations.

REFERENCES

1. F. M., Burdekin, Proc. Instn. Civ. Engrs Structs. & Bldgs. 99, 89 (1993).
2. "Potential drop nondestructive testing," in *Nondestructive Testing Handbook*, Vol. 9, eds. R. K. Stanley, P. O. Moore, and P. McIntire (ASNT, Columbus, 1995), pp. 378-397.
3. R. Ghajarieh, M. Saka, H. Abe, I. Komura, and H. Sakamoto," NDT&E Int. 28, 23 (1995)
4. M. Saka, K. Hara, H. Abe, JSME Series A: Mech. Mater. Engin. 38, 273 (1995).
5. S., Nath, Electrosoft 2, 92 (1991).
6. J. Gu and L. Y. Yu, NDT Int. 23, 161 (1990).
7. H. H. Johnson, Mater. Res. Stand. 5, 442 (1965).
8. A. Uhlir, Bell Syst. Techn. J. 23, 105 (1955).
9. R. O. Ritchie and K. J. Bathe, Int. J. Fract. 15, 47 (1979).
10. ANSYS User's Manual, ANSYS Version 5.2, SAS IP, 1995.
11. Y. Ke and P. Stahle, Int. J. Num. Meth. Eng. 36, 3205 (1993).